doi:10.2533/chimia.2025.433 Chimia 79 (2025) 433–440

A Scalable Dynamic Cascade Flow Reactor for Challenging Continuous Heterogeneous Processes

Kim-Long Diep[a], Emilie Buchs[a], Marlies Moser[b], Finn L. Steinemann[b], Alain G. Georg[b], Flavien L. Morel[c], Michal Dabros[a], and Roger Marti[a]*

Abstract: Continuous processes (often referred to as flow chemistry) offers multiple advantages over batch processes and are of particular interest for industrial applications as they provide a more direct path towards process intensification, increased safety and efficiency. However, some chemical processes are still challenging to run in a continuous fashion, such as reactions producing fouling, using stoichiometric amounts of solids, or requiring long residence times. For those kinds of reactions, batch approaches are usually preferred even though some processes would still benefit from the advantages inherent to flow. We herein report our testing and development of a scalable continuous flow reactor equipped with active mixing that was designed to handle those challenging continuous processes, such as the continuous formation of a Grignard reagent from a magnesium powder slurry.

Keywords: Continuous processes · CSTR · Flow chemistry · Solids · Suspensions

From left to right: Kim-Long Diep, Flavien Morel, Emilie Buchs, Roger Marti, Finn Steinemann, Michal Dabros, Marlies Moser. Missing: Alain Georg.

Dr. Kim-Long Diep studied chemistry at the University of Fribourg, where he obtained his Master's degree in 2017 in synthetic organic photochemistry under the guidance of Prof. Christian G. Bochet. He remained in the Bochet group to carry out a PhD thesis on oligonucleotide templated reactions, which he completed in 2021. He then worked as a Process R&D Chemist at Siegfried Evionnaz before moving back to Fribourg at the HEIA-FR as an Academic Associate to work on flow chemistry projects.

Emilie Buchs studied chemical engineering at the HEIA-FR, where she obtained her Bachelor's degree in 2022. She then stayed at the institute to do a Master's in Chemical Development and Production while working part time on various research projects as an Academic Associate. Currently, Emilie is carrying out her Master's Thesis in the group of Prof. B. Lipshutz in UC Santa Barbara.

Marlies Moser studied biotechnology at the ZHAW Wädenswil and chemistry at the ETH Zurich. She completed her Master's thesis in 2016 in the Wennemer's group, where she worked on the synthesis of collagen model peptides. In 2017, she joined Fluitec mixing + reaction solutions AG, where she works in the sales and R&D team.

Finn Steinemann studied chemistry at the ZHAW Wädenswil and specialized in flow chemistry. He worked as a research assistant at the ZHAW before joining Fluitec mixing + reaction solutions AG in the R&D department in 2022.

Alain Georg graduated in 1991 as a mechanical engineer from the Zurich University of Applied Sciences. He began his career as a project and sales engineer for polymers. In 1993 he founded the company Fluitec AG. The main products of Fluitec were initially static mixers and mixer heat exchangers, before Fluitec became more and more active in reaction technology and today offers a wide range of products for flow chemistry. As head of the R&D team, Alain Georg has been intensively involved in the safety engineering of continuous reactors for the last 10 years.

Dr. Flavien L. Morel studied chemical engineering at the Ecole Polytechnique Fédérale de Lausanne. He obtained his PhD with Prof. Dr. J. A. van Bokhoven at the ETH Zurich. He joined Firmenich SA (now dsm-firmenich) in 2016 as a Scientist where his research focuses on novel reaction technologies and continuous processing.

Dr. Michal Dabros studied chemical engineering at the University of Alberta (BSc) and Polytechnique Montréal (MSc). He completed his PhD degree in the field of bioprocess engineering, under the guidance of Prof. Dr. U. von Stockar at EPFL Lausanne. Following a postdoctoral position at Dublin City University, he joined the HEIA-FR in 2010, where he works as an associate professor of chemical engineering and process control. His main areas of interest include Process Analytical Technologies (PAT), focusing on on-line monitoring, simulation, control and optimization of chemical and upstream biotech processes.

*Correspondence: Dr. R. Marti, E-mail: roger.marti@hefr.ch
[a]Institute of Chemical Technology, Haute école d'Ingénierie et d'Architecture Fribourg, HES-SO University of Applied Sciences and Arts Western Switzerland, Boulevard de Pérolles 80, CH-1700 Fribourg, Switzerland; [b]Fluitec mixing + reaction solutions AG, Seuzachstrasse 40, CH-8413 Neftenbach; [c]dsm-firmenich, Route de la Plaine 125, CH-1283 Dardagny

Dr. Roger Marti is a Full Professor UAS of Organic Chemistry & Process Chemistry at the Institute ChemTech at the HEIA-FR. His research interests and competences are in synthetic organic chemistry & process chemistry for the synthesis and sustainable production of functional organic molecules and polymers using innovative synthesis technologies.

1. Introduction

1.1 *Flow Chemistry – A Powerful Synthetic Tool with a Solid Problem*

Over the last decades, flow chemistry[1] has established itself as a powerful method that allows a precise control over chemical processes in time and space. When compared to batch approaches, flow systems can offer attractive benefits such as increased heat transfer rates thanks to higher surface to volume ratios, faster reaction times thanks to easy access to above boiling point of solvent temperatures, a smaller footprint and a generally easier path towards process intensification.[2] For these reasons, continuous processes are of particular interest for industry. However, not all chemical processes are easily carried out in flow: reactions requiring stoichiometric amounts of solid reagents or that are prone to fouling are challenging to run in conventional flow reactors, both at laboratory and industrial scales. In such processes batch is typically preferred to prevent pipe clogging with solids, although most processes would in fact benefit from the aforementioned advantages of flow. This was demonstrated in a study of various processes at Lonza by Roberge *et al.*[3] where around half the reactions studied would have benefited from flow chemistry. However, around 63% of those reactions contained solids and could not be carried out in microreactors. Reactions that are prone to produce fouling such as organolithiations[4] can also be problematic to perform over long periods of time due to formation of lithium hydroxide salts. This can be avoided by drying the solvents, which in turn negatively impacts productivity due to the additional operations and in-process controls required.

Another challenging class of reactions to run in flow are slow reactions, which require long residence times to reach high conversions. In larger pipes, static mixers are required to improve the mixing of reagents which is crucial for processes limited by mass transfer. For static mixers to be efficient, a sufficient flowrate needs to be used to ensure efficient mixing. For reactions with slow kinetics, this makes the common tubular flow reactor an unsuitable option, as an unreasonably long piece of equipment would be required to achieve a long residence time with suitable mixing due to minimum flowrate requirements.

Multiple strategies offer viable options to handle solids in continuous processes.[5] Oscillatory flow can be used to keep particles suspended when travelling along pipes.[6–9] Packed bed reactors are an attractive option, especially for heterogeneous catalytic processes. However, solid reagents used in stoichiometric amounts will deplete quickly and inevitably require a replenishing of the packed bed. Another common approach is to use available batch equipment as semi-batch systems or continuously stirred tank reactors (CSTR), which combines the ability of batch reactors to handle particles in suspension and some of the advantages of classical tubular continuous systems. Still, CSTRs are not without drawbacks. Cascades of a large number of CSTRs are required to reach high Bodenstein numbers and thus plug-flow like residence time distribution, which is readily offered by classical plate or coiled reactors using a smaller footprint. To implement CSTRs in flow systems on a laboratory scale, multiple miniature CSTR systems[10–12] have been developed in the more recent years and are available commercially or open-source.[10,13] Kapur *et al.* reported in 2017 their simple and versatile laboratory scale CSTR system, the fReactor[10] which is now commercially available from Asynt (Cambridgeshire, United Kingdom). We have recently reported our design of a mini CSTR,[13] which is equipped with a jacket for heating/cooling. This mini CSTR is capable of handling multiphasic reactions (solid/liquid, gas/liquid) thanks to the implemented mechanical stirring and supports various accessories such as Process Analytical Technology (PAT) and temperature probes. Prototypes of CSTR cascades have been reported,[14] and larger CSTR systems can also now be obtained commercially[15] although the technology is still not widely available. We herein report our testing and development of a new CSTR cascade reactor system manufactured by Fluitec mixing + reaction solutions AG (Neftenbach, Switzerland), which was designed to handle heterogeneous and homogeneous chemical processes that would be challenging to run in conventional flow reactors.

1.2 *Fluitec's Dynamic Cascade Reactor*

The Dynamic Cascade Reactor (DCR), built and developed by Fluitec mixing + reaction solutions AG (Neftenbach, Switzerland), is a continuous reactor equipped with active mixing which acts as a cascade of 12 CSTR with a total volume of 420 mL (see Fig. 1 for full specifications). The DCR was designed to perform challenging continuous processes such as reactions that are multiphasic, prone to fouling or that require long residence times. The mixing elements on the rotating shaft are fully customizable, making the reactor modular and adaptable to a wide range of processes. Jackets with multiple injection points along the reactor length are also available for crystallization applications or processes requiring multipoint injections (see Fig. 5 in part 2.2).

2. Reactor Characterization

2.1 *Residence Time Distribution Analysis*

Residence time distribution (RTD) analysis was performed using a sodium chloride tracer and conductivity measurements (pulse method). A design of experiment (DoE) using the software MODDE 13 (Sartorius, Göttingen, Germany) was performed to produce a model of the residence time distribution, using flowrates (10 – 50 mL min^{-1}) and stirring speeds (30 – 1000 rpm) as factors. The DoE analysis indicated that flowrate and flowrate squared were the only statistically relevant parameters for mean residence time modelling. Along with mean residence times, the variance of each distribution measured was calculated and was used to calculate Bodenstein numbers (Bo) for each scenario. From the residence time distribution curves and those Bodenstein numbers, the effective theoretical number of CSTR in a cascade for each scenario can also be calculated. The residence time mod-

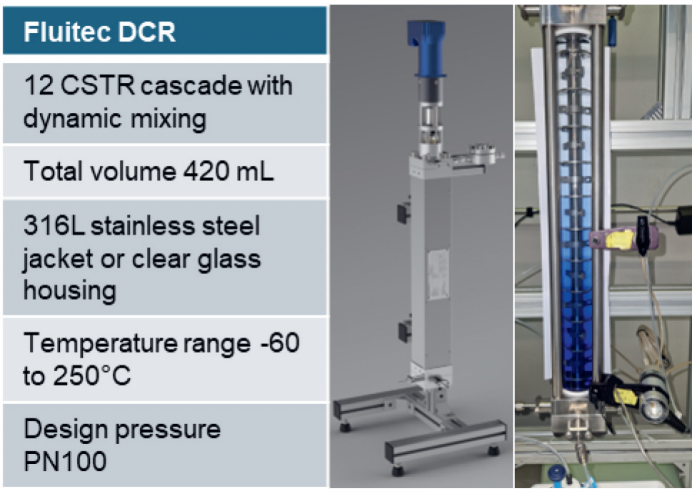

Fig. 1. Left to right: specifications of the Fluitec DCR, Fluitec DCR (metal housing), Fluitec DCR (glass housing).

el, detailed methodology and equations used for the RTD characterization are available in the supporting information (SI).

As expected, the stirring speed has a major effect on the shape of the residence time distribution curve (Fig. 2, see SI for additional curves). Higher stirring speeds increase the amount of back mixing in the DCR and result in lower Bodenstein numbers (Fig. 3, 3 – 10 Bo). This strong back mixing can be somewhat diminished if higher flowrates are applied but cannot be completely suppressed. At lower stirring speeds however, Bodenstein numbers in the ranges of 30 to 40 can be reached and a plug-flow like distribution is observed. Higher numbers can theoretically be reached by either connecting multiple DCRs in series or by making smaller mixing chambers in the DCR, thus increasing the number of physical mixing chambers in the reactor. It is worth noting that at high flowrates and low stirring speeds, the DCR effectively behaves like a cascade of a higher number of CSTRs than its 12 physical chambers (Fig. 4).

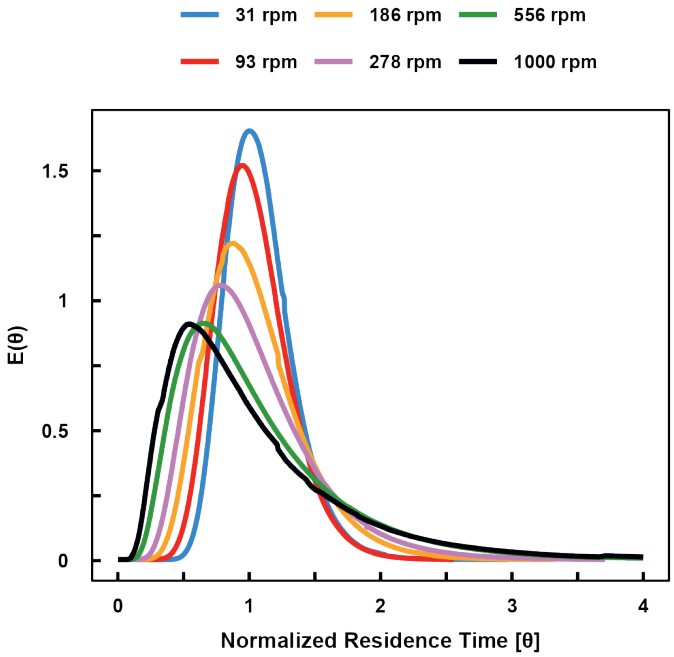

Fig. 2. Dimensionless residence time distribution curves for a flowrate of 30 mL/min at various stirring rates.

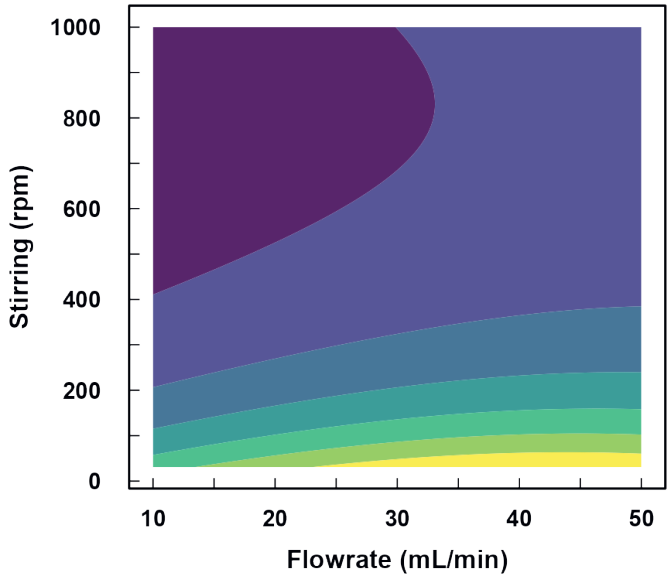

Fig. 3. Contour plot describing Bodenstein numbers (Bo) as a function of stirring and flowrate.

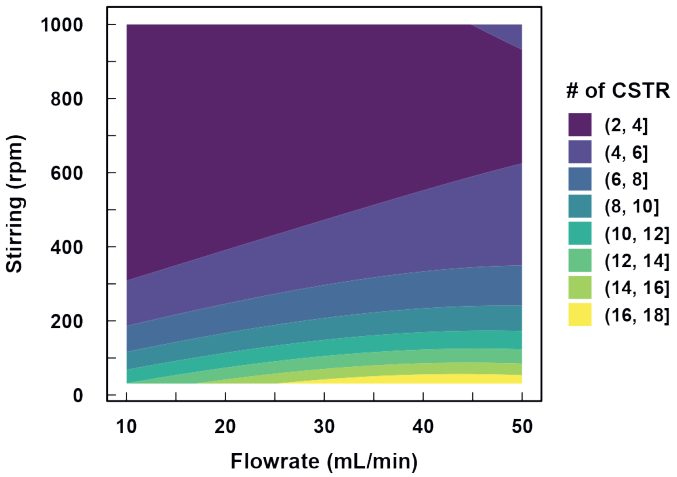

Fig. 4. Contour plot describing the theoretical CSTR cascade numbers as a function of stirring and flowrate.

2.2 *Thermal Characterization*

The overall heat transfer coefficient (k) was determined by heating experiments involving isopropyl alcohol, raising the temperature from room temperature to 60 °C in the DCR. The jacket of the DCR was operated with water at a constant temperature and a high mass flow rate to maintain isoperibolic conditions. Several heating curves were measured by varying stirring speeds between 0 and 980 rpm and flow rates between 20 and 400 mL/min as both parameters have an influence on convection and thus on the heat transfer. Multiple temperature measurements along the tube enabled evaluation of the heating curve and deduction of the k values by segment-wise analysis.[16] The temperature measurement ports could also serve as multiple injection ports for cascaded dosing (Fig. 5).

Similar to the description in Zlokarnik[17] (Eqn. 1), an empirical Nu function has been deduced. The proposed correlation (Eqn. 2) is valid for volumetric flow rates between 20 and 200 mL/min, stirring speeds between 50 and 800 rpm and Reynolds

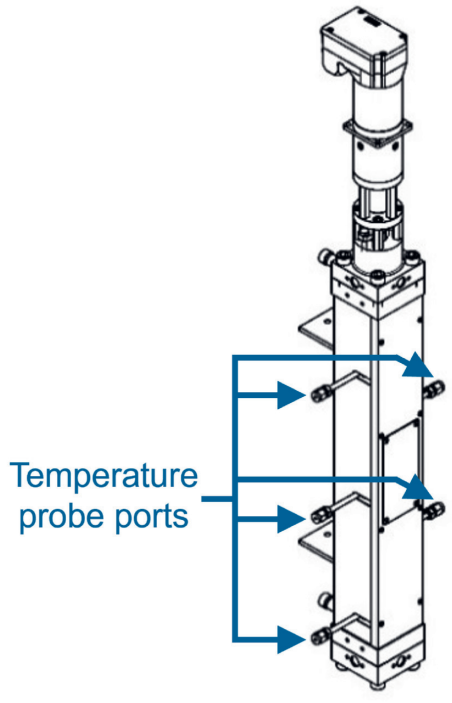

Fig. 5. DCR for thermal analysis with 5 temperature probe ports along the tube which could also serve as multiple injection ports for cascaded dosing.

numbers (Re) between 200 and 8000 for the DCR described herein.

$$Nu = const \cdot Re^{\frac{2}{3}} \cdot Pr^{\frac{1}{3}} \cdot \left(\frac{\eta_W}{\eta}\right)^{-0.14} \quad (1)$$

$$Nu = 0.0176 \cdot \left(\frac{\dot{V}}{\dot{V}_{ref}}\right)^{0.5546} \cdot Re^{\frac{2}{3}} \cdot Pr^{\frac{1}{3}} \cdot \left(\frac{\eta_W}{\eta}\right)^{-0.14} \quad (2)$$

Where $\dot{V}$ is the flowrate given in mL/min, $\dot{V}_{ref}$ the reference flowrate of 1 mL/min, η corresponds to the viscosity in the core flow and η_W to the viscosity at the wall. The formulae for *Re* and *Pr* are described in the SI, as are details on how *k* is calculated from *Nu*. The *Nu* function was chosen rather conservatively, *i.e.* the predicted *k* values are lower than the measured *k* values (Fig. 6). This is favourable for the process engineering design of the reactor.

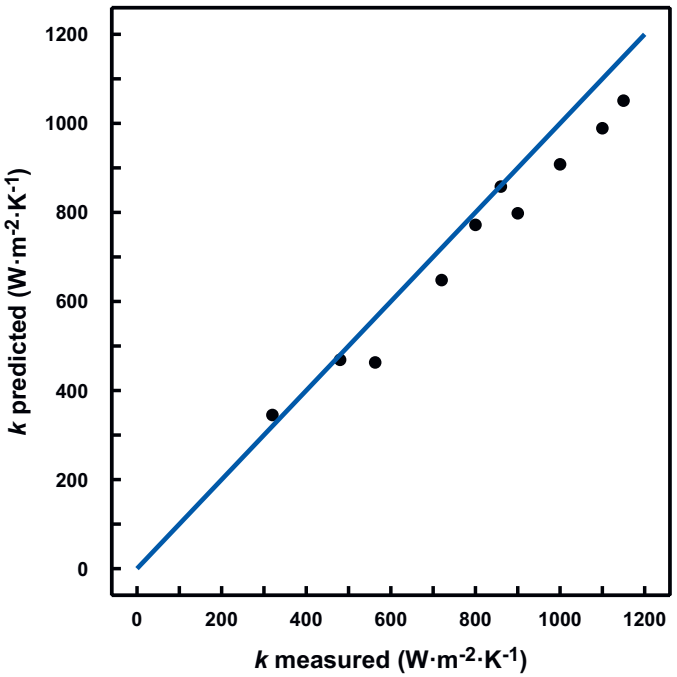

Fig. 6. Presentation of the k values calculated out of the *Nu* function (predicted) against measured k values.

The heat transfer characteristics of the DCR are compared with those of static mixers in Table 1. As feed solutions are usually limited and expensive, small flow rates (~ 20 mL/min) are preferable. In contrast to the static mixer, there is an additional energy input in the DCR due to the stirrer, which enhances the heat transfer. While at 20 mL/min the *k* value of a static mixer with the same diameter (36 mm) is 6-times lower than with the DCR at high stirring speed (977 rpm), comparable *k* values are achieved using the lab-scale static mixer with a diameter of 7.8 mm. However, a 20-times shorter residence time is obtained in the 7.8 mm static mixer compared with the DCR. The DCR is therefore suitable for laboratory reactions with a long residence time, whereas the static mixer is suitable for very fast exothermic reactions due to its very high specific heat transfer capacity. At similar heat transfer, the specific heat transfer capacity of a static mixer is approximately 9-times higher compared to the DCR.

Table 1. Comparison of the heat transfer characteristics of the DCR and static mixer.

	DCR	Static mixer	
Internal diameter (mm)	36	36	7.8
Length (mm)	500	500	500
Volume (mL)	420	465	17
Flow rate (mL/min)	20	20	20
Stirring speed (rpm)	977	–	–
Residence time (min)	21	23	1
Overall heat transfer coefficient *k* (W/m²/K)[a]	345	55	429
Specific heat transfer capacity (W/K/L)[b]	54	9	494

[a]Calculated using Fluitec software no. 92-27005.
[b]Calculated using Fluitec software no. 92-30001.

3. Continuous Emulsion Polymerization

Emulsion polymerization is used to produce polymers with high molecular weights to be used in a variety of applications such as coatings, adhesives and the preparation of synthetic rubbers.[18,19] The most common type of emulsion polymerization is the 'oil in water' type, where droplets of neat monomer stabilized by a surfactant are polymerized using a water soluble radical initiator.[20] At the end of the reaction, a latex (suspension of polymer droplets in water) is obtained and the polymer has to be used as such or it must be separated from the water and additives before further processing. Acrylates and styrenes are the monomers of choice for emulsion polymerization. Emulsion polymerizations can be problematic to run in tubular reactors, as the process is very prone to fouling through various pathways,[21,22] leading to pipe cloggages over time.[23] Moreover, a relatively long residence time (~20 to 60 min) is usually required, which exacerbates the fouling aspects. Sufficient mixing is also paramount to sustain the emulsion. Reactors equipped with static mixers are thus not ideal to perform such processes, as they require a certain minimal flowrate to mix efficiently. With the relatively long residence time associated with emulsion polymerization, this would lead to an unreasonably large equipment size necessary to run such polymerizations. Semi-batch or loop reactors can be used to mitigate some of the problems mentioned above.[23]

With its active mixing, we hypothesized that the DCR would be well suited to carry out emulsion polymerizations with limited fouling. Proof of concept experiments were carried out to visually assess the amount and main locations of fouling in the reactor over approximately 5 hours of reaction. An oil in water type polymerization of butyl acrylate was chosen as the test candidate, as it gave the most fouling issues during our prelimi-

Table 2. Reaction conditions for the qualitative fouling experiment in the DCR. Concentrations correspond to the solution formed inside the reactor after mixing the two inlet feeds.

Monomer	20 wt% butyl acrylate in water
Surfactant	2 wt% SDBS
Initiator	1 wt% potassium persulfate
Jacket temperature	65 °C
Total flowrate	6 mL/min
Stirring	1000 rpm

nary experiments in batch (Table 2). The initial emulsion (water, monomer, and surfactant) was generated in a separate tank and kept under vigorous stirring over the reaction time prior to its introduction in the DCR using a peristaltic pump. The initiator was solubilized in deionized water in a second container and was introduced through another inlet of the reactor also using a peristaltic pump.

After the reaction, the reactor was rinsed and inspected for fouling. Fouling mainly occurred at the extremities of the stirring shaft (Fig. 7) close to the inlets at the bottom and the outlets at the top. The rest of the stirring shaft and the jacket exhibited minimal to visually undetectable fouling. Emulsion polymerizations using static mixers produced a much larger amount of fouling. The impact of other relevant parameters such as polymer molecular weight and latex particle sizes are outside the scope of this work.

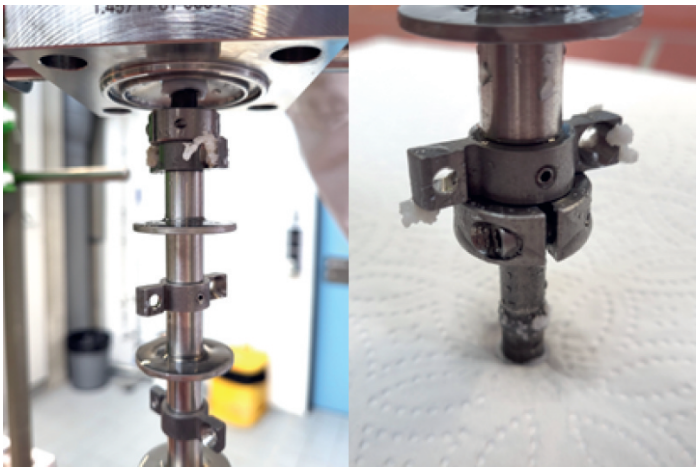

Fig. 7. Stirring shaft after emulsion polymerization (left: top of the shaft, right: bottom of the shaft).

4. Continuous Aqueous Stahl-Hoover Oxidation

To test the DCR's capabilities with gas-liquid systems, we settled on the Stahl-Hoover[24–26] oxidation (Copper-TEMPO mediated) as a test reaction, with benzyl alcohol as the test substrate (Scheme 1 and Table 3). In order to work safely with air as the oxygen source for the reaction, we adapted a procedure[27] from Lipshutz and coworkers using an aqueous medium in the presence of a surfactant (TPGS-750M[28]) instead of pure acetonitrile. During the tests studies in batch prior to carrying out the reaction in flow, we ran into the issue of excess foaming when bubbling air in the reaction medium. It was found that the addition of 5 vol% of acetonitrile greatly reduced the formation of foam while still keeping the flash point of the reaction below the working temperature.

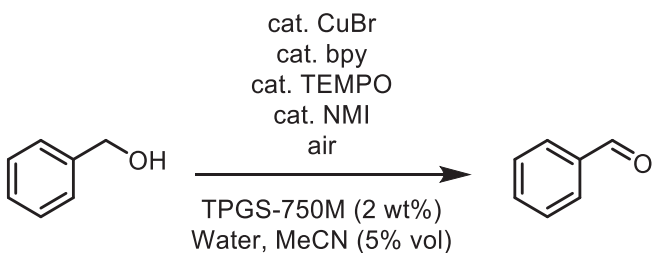

Scheme 1. Stahl-Hoover oxidation of benzylic alcohol.

Through a variety of tests in batch mode, it was found that at room temperature and ambient pressure the reaction was in most applicable cases kinetically limited rather than mass transfer limited. A relatively high amount of catalyst of 0.1 equivalent (relative to the benzyl alcohol) was thus used to obtain reasonable reaction kinetics, where full conversions could be reached in about 90 minutes in small scale batch mode during our initial tests. When attempting the reaction using the same conditions in flow using the DCR (experimental setup available in the supporting information) at a flowrate of 4.2 mL/min, corresponding to a residence time of approximately 100 minutes, we achieved only 80% conversion. Lowering the total flowrate to 2.5 mL/min enabled us to obtain the expected full conversion. After investigation, it was found that under those conditions the reactor only held about 217 mL of liquid instead of 420 mL. This meant that under those conditions a residence time of about 60 minutes was obtained using the initial flowrate instead of the targeted 100 minutes, which explained the lower conversion when compared to our initial tests in batch mode. This lower liquid volume is due to the very high air flowrate compared to the liquid flowrate (~96% of the total volume of the fluid introduced was air), and thus the presence of a volume of air in the reactor is unavoidable under those conditions, especially at high stirring intensities. Static mixer based systems would also show a lowered liquid volume under such a high air to liquid flowrate ratio.

Table 3. Reaction parameters used for the continuous Stahl-Hoover oxidation.

Reaction concentration	0.5 M
Air flowrate	100 mL/min
Total liquid flowrate	4.2 mL/min
Jacket temperature	21 °C
Pressure	ambient
Stirring	900 rpm

With the corrected residence time, the oxidation reaction thus seems to perform similarly in flow or in batch. Further work will be carried out to investigate the effect of pressure and temperature on the reaction kinetics. Additionally, different stirrer geometries are also being investigated to increase the liquid hold-up and improve gas-liquid mass transfer.

5. Continuous Grignard Reagent Formation

To illustrate the DCR's ability to handle the presence of solids, we decided to synthesize a Grignard reagent from a slurry of magnesium powder in 2-methyltetrahydrofuran (2-MeTHF). The Nobel prize winning Grignard reaction[29] is still used extensively to create C-C bonds in a vast array of processes for fine chemicals.[30] Grignard reagents are typically prepared industrially under batch conditions,[31] but continuous systems have been developed in the last decades.[31–37] CSTRs have been employed to produce Grignard reagents on multi kilogram scale.[36,37] Due to the difficulty of handling solids in flow reactors, most reported continuous synthesis of Grignard reagents use packed bed reactors containing a cartridge of magnesium turnings/powder. Well activated magnesium is required for those packed-bed type reactors in order to ensure that the reaction will proceed during the residence time, so those reactors can only run for a fixed amount of time due to the stoichiometric consumption of the magnesium bed during the reaction. Common chemical options[38] to activate magnesium are iodine, 1,2-dibromoethane, DIBAL-H or Grignard reagents themselves. Menges-Flanagan and coworkers from the Fraunhofer Institute developed[31,34,35] a continuous reactor where magnesium turnings can be fed from the top of the reactor to run in a fully continuous fashion. The fed magnesium is activated mechanically by grinding, which ensures that the reaction will proceed swiftly. Our approach to continuously prepare a Grignard reagent in the DCR was to pre-activate 20–230 mesh magnesium and pre-fill the

reactor with about one equivalent of the metal powder suspended in 2-MeTHF. The suspension is then heated, and the halide in solution is introduced into the reactor from one inlet (see Fig. 8 for the experimental setup used). Another inlet is used to introduce a slurry of fresh magnesium powder in 2-MeTHF, with a molar flowrate matching that of the halide's to ensure that the amount of magnesium in the reactor stays as constant as possible. We hypothesized that thanks to the active agitation, there would be sufficient back-mixing in the vessel for the formed Grignard reagent to further activate the fresh magnesium entering the system, thus sustaining the reaction throughout the reactor's volume. The produced Grignard reagent would then be collected and directly quenched in a thermostated reactor containing an aqueous ammonium chloride solution.

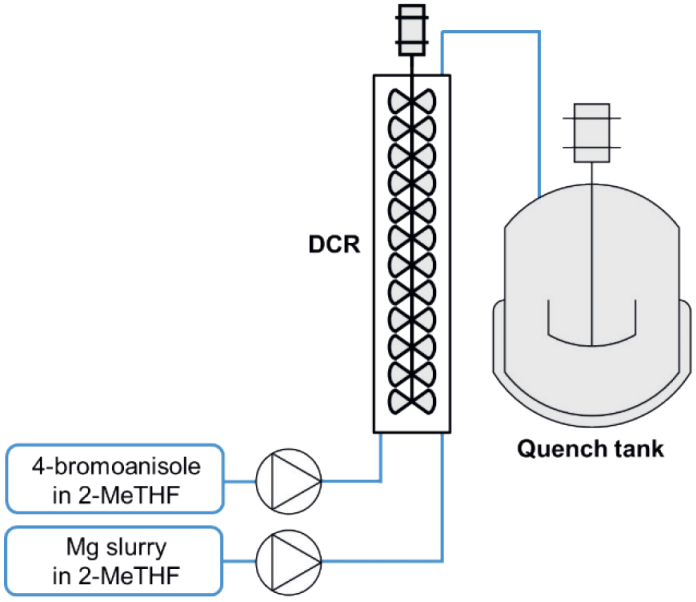

Fig. 8. Experimental setup for the Grignard reagent formation.

It is worth noting that pumping suspensions at a fixed molar flowrate is not a trivial task for multiple reasons, mainly the settling of the solids in the transfer lines, and the difficulty of maintaining homogeneity of the stirred suspension in the feeding tank. The choice of a usable pump for such an application is also quite limited since it must be able to handle the presence of solid particles as well as 2-MeTHF which was found to be incompatible with most tubing material used in peristaltic pumps. The relatively low flowrate used for this experiment (10 - 20 mL/min) also prohibits the use of industrial centrifugal pumps, which would be a common choice to pump such slurries.

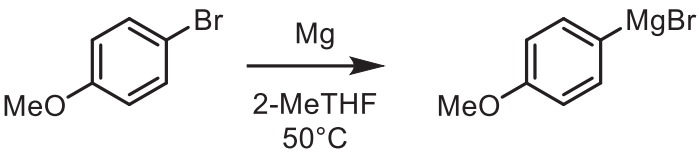

Scheme 2. Synthesis of 4-methoxymagnesium bromide.

We chose 4-bromoanisole as the test halide (Scheme 2), as it is less prone to common side reactions in Grignard reagent formation (*e.g.* Wurtz coupling). Furthermore, 4-bromoanisole and its post-reaction quenching product anisole are easily quantifiable by GC-FID or NMR.

5.1 *Grignard Reagent Formation – Thermal Safety*

As the formation of a Grignard reagent and its quench are known to be highly exothermic, we first studied the thermal safety of the process in order to guide us into safe reaction parameters prior to any experimentation in flow. The reaction enthalpy of the Grignard reagent formation and its quench were measured using the RC1mx reaction calorimeter from Mettler-Toledo. The reaction enthalpy measured experimentally for the formation of 4-methoxyphenylmagnesium bromide from 4-bromoanisole and magnesium was -295 kJ/mol, which matches well with reported reaction enthalpies of other Grignard reagents in the literature.[39,40] For the quench with water, an enthalpy of -352 kJ/mol was obtained. From those values, we decided to start our investigations targeting a relatively low concentration of around 0.16 M in the DCR, which would result in a safe adiabatic temperature raise (ΔT_{ad} = 31°C) to carry out our first tests.

5.2 *Continuous Grignard Reagent Synthesis – Results and Discussion*

As mentioned in the previous thermal safety section, we first started our investigation at a relatively low halide concentration of 0.16 M of halide in the reactor to get a feeling of the heat transfer and jacket response during the reaction. Pre-activation of the magnesium suspension in 2-MeTHF was performed using 1 mol% (relative to magnesium) of either commercial DIBAL-H solution in toluene or 4-methoxyphenylmagnesium bromide in THF. Both activation methods gave similar results overall. Samples of the produced reagent were collected every 10 minutes and quenched in an ammonium chloride solution to monitor the conversion of 4-bromoanisole to the Grignard reagent. The release of heat corresponding to the start of the reaction could be observed when monitoring the temperature at the outlet of the jacket.

For the experiments at a lower concentration, 4-bromoanisole was converted rather slowly into the Grignard reagent and required extended time to reach maximum conversion. Full conversion could not be reached in a reasonable amount of time during our first attempt (Table 4, Entry 1), and to remedy this issue we decided to increase the initial amount of magnesium in the reactor in order to accelerate the reaction. This was partially successful, as shown in Entry 2 where full conversion of 4-bromoanisole was reached after 50 minutes. Any further samples later collected during that experiment were then fully converted, but obvious downsides of this approach are that a larger excess of magnesium is required and that the first 50 minutes of reagent solution produced will be impure due to the presence of unreacted starting material. A more efficient approach was then found when running the reaction at a higher concentration (and lower flowrate to avoid pump clogging), where a portion of the halide solution in 2-MeTHF was introduced into the reactor and was left to react in batch mode for 30 minutes to ensure that the magnesium inside the reactor would be fully activated. After this activation period the pumps were restarted and 4-bromoanisole was absent in every sample collected at the outlet of the reactor. This approach was repeated with the lower concentration reaction at higher flowrate to check if the reaction would still be fast enough under those conditions and it gave similar results (Entry 4).

With the ability to perform the magnesium activation in batch mode prior to starting the flow process, we also investigated if any pre-activation was necessary, as well as if dry 2-MeTHF was required for the process to run smoothly. The same procedure and reaction conditions from Entry 3 were used again in Entry 5 with technical grade 2-MeTHF that was not submitted to any drying agent. Additionally, no pre-activation was performed on the magnesium powder. After pre-loading the magnesium in the reactor, a portion of the halide was introduced and left to react in batch mode similarly to Entry 3. However, no exotherm could be detected from the jacket temperature measurements, indicating that the desired

Table 4. Results summary of the continuous Grignard reagent formation experiments. All reactions were performed with a jacket temperature set to 50 °C. 2-MeTHF was dried over molecular sieves (<50 ppm water content).

Entry	Total flowrate (mL/min)	Halide concentration in the reactor (M)	Amount of magnesium pre-loaded in the reactor (equiv)	Conversion in the outlet stream after 20 minutes	Time to reach 100% conversion in the outlet stream (min)
1	20	0.16	2.7 g (0.6 equiv)	20%	N.A.
2	20	0.16	4.7 g (1.0 equiv)	29%	50
3[a]	12	0.5	6.0 g (0.7 equiv)	100%	Immediate
4[a]	20	0.16	3.1 g (0.7 equiv)	100%	Immediate
5[a,b]	12	0.5	6.0 g (0.7 equiv)	100%	Immediate

[a]0.1 equiv of the halide was introduced in the reactor and left to react in batch until no more exothermicity was observed prior to starting the pumps (batch initiation method).

[b]Technical 2-MeTHF was used (~1500 ppm water content, no prior drying) and no activation procedure was initially performed on the magnesium suspension.

Grignard reagent formation was either not occurring at all or that the reagent was forming at a very slow rate. It was then possible to initiate the reaction by injecting 1 mol% of DIBAL-H solution (relative to the total amount of magnesium used) directly in the DCR, which instantly triggered a response from the jacket due to the heat released. When no more noticeable exotherm was detected, the pumps were restarted and 4-bromoanisole was again absent in all of the collected samples. It is thus likely that the magnesium activation step is still crucial to ensure a rapid reaction initiation, but the use of undried technical solvents does not cause any practical problem for the reaction system. It is worth mentioning that although no experimental issue was observed using undried technical solvents, any water in the system will react with the formed Grignard reagent, decreasing the actual yield and potentially forming additional impurities during the following addition step.

6. Conclusion and Outlook

In summary, we have reported the characterization and application tests of a new commercially available dynamic cascade flow reactor. The reactor is highly modular, with the possibility to fine-tune mixing elements along the stirring shaft or to apply cascaded dosing to accommodate a wide range of processes. The reactor has already been scaled-up to a 100 L version. The reactor was used successfully for processes that are usually more challenging to run in flow such as emulsion polymerizations that are prone to fouling. Gas-liquid reactions can also be carried out in the reactor, although with a diminished overall liquid volume. We expect that this will be improved in a future version of the stirring unit, with a geometry better suited to increase the liquid hold-up in the reactor.

It was also shown that the reactor performs well in solid-liquid reactions, as shown in its ability to carry out Grignard reagent formations with powdered magnesium metal. This final application is of particular interest, as few production scale continuous reactors exist to perform such reactions in a similar fashion. More specialized systems are available from various companies to produce Grignard reagents, but the DCR looks to be a viable and likely more versatile option than some commercially available systems.

Acknowledgements

We greatly thank the financial support from the Innosuisse program (104.458 IP-ENG). The technical support from Mr. Michel Audriaz (HEIA-FR) and Mr. Eric Clément (HEIA-FR) and Mr. Rémy Simonin (HEIA-FR) is greatly acknowledged. We thank Dr. Fabrice Gallou (Novartis) for the generous donation of the TPGS-750-M required for the oxidation experiments.

Supporting Information

Additional information on residence time distribution determinations, thermal characterization of the DCR, and application tests are available free of charge at www.chimia.ch/chimia/article/view/2025_433.

Received: February 22, 2025

[1] M. B. Plutschack, B. Pieber, K. Gilmore, P. H. Seeberger, *Chem. Rev.* **2017**, *117*, 11796, https://doi.org/10.1021/acs.chemrev.7b00183.
[2] C. D. Risi, O. Bortolini, A. Brandolese, G. D. Carmine, D. Ragno, A. Massi, *React. Chem. Eng*. **2020**, *5*, 1017, https://doi.org/10.1039/D0RE00076K.
[3] D. M. Roberge, L. Ducry, N. Bieler, P. Cretton, B. Zimmermann, *Chem. Eng. Technol*. **2005**, *28*, 318, https://doi.org/10.1002/ceat.200407128.
[4] P. Filipponi, F. Venturoni, R. Suremann, A. Streit, S. Schoenebeck, B. Schenkel, J. Polenk, L. Piccioni, R. O'Meadhra, S. Mostarda, J. Haber, B. Guelat, S. Wegmann, *CHIMIA* **2019**, *73*, 809, https://doi.org/10.2533/chimia.2019.809.
[5] H. L. D. Hayes, C. J. Mallia, *Org. Process Res. Dev*. **2024**, *28*, 1327, https://doi.org/10.1021/acs.oprd.3c00407.
[6] B. J. Doyle, G. Vrbanec, C. Aellig, E. Marcelić, S. Filliger, A. Macchi, D. M. Roberge, *Org. Process Res. Dev*. **2024**, *28*, 1929, https://doi.org/10.1021/acs.oprd.3c00476.
[7] B. J. Doyle, B. Gutmann, M. Bittel, T. Hubler, A. Macchi, D. M. Roberge, *Ind. Eng. Chem. Res*. **2020**, *59*, 4007, https://doi.org/10.1021/acs.iecr.9b04496.
[8] T. McGlone, N. E. B. Briggs, C. A. Clark, C. J. Brown, J. Sefcik, A. J. Florence, *Org. Process Res. Dev.* **2015**, *19*, 1186, https://doi.org/10.1021/acs.oprd.5b00225.
[9] M. Jiang, X.-W. Ni, *Org. Process Res. Dev*. **2019**, *23*, 882, https://doi.org/10.1021/acs.oprd.8b00446.
[10] M. R. Chapman, M. H. T. Kwan, G. King, K. E. Jolley, M. Hussain, S. Hussain, I. E. Salama, C. González Niño, L. A. Thompson, M. E. Bayana, A. D. Clayton, B. N. Nguyen, N. J. Turner, N. Kapur, A. J. Blacker, *Org. Process Res. Dev*. **2017**, *21*, 1294, https://doi.org/10.1021/acs.oprd.7b00173.
[11] Y. Mo, K. F. Jensen, *React. Chem. Eng*. **2016**, *1*, 501, https://doi.org/10.1039/C6RE00132G.
[12] A. Pomberger, Y. Mo, K. Y. Nandiwale, V. L. Schultz, R. Duvadie, R. I. Robinson, E. I. Altinoglu, K. F. Jensen, *Org. Process Res. Dev.* **2019**, *23*, 2699, https://doi.org/10.1021/acs.oprd.9b00378.
[13] U. Gnädinger, D. Poier, C. Trombini, M. Dabros, R. Marti, *Org. Process Res. Dev*. **2024**, *28*, 1860, https://doi.org/10.1021/acs.oprd.3c00424.
[14] F. Mandrelli, A. Buco, L. Piccioni, F. Renner, B. Guelat, B. Martin, B. Schenkel, F. Venturoni, *Green Chem*. **2017**, *19*, 1425, https://doi.org/10.1039/C6GC02840C.
[15] N. Cherkasov, S. J. Adams, E. G. A. Bainbridge, J. A. M. Thornton, *React. Chem. Eng*. **2023**, *8*, 266, https://doi.org/10.1039/D2RE00232A.
[16] M. Moser, A. G. Georg, F. L. Steinemann, D. P. Rütti, D. M. Meier, *J. Flow Chem*. **2021**, *11*, 691, https://doi.org/10.1007/s41981-021-00204-y.
[17] M. Zlokarnik, 'Rührtechnik', Springer, Berlin, Heidelberg, **1999**, https://doi.org/10.1007/978-3-642-58635-4.

[18] H. Tobita, A. E. Hamielec, in 'Polymerization Processes, 2. Modeling of Processes and Reactors, Ullmann's Encyclopedia of Industrial Chemistry', John Wiley & Sons, Ltd, **2015**, p. 1, https://doi.org/10.1002/14356007.o21_o01.pub2.
[19] C. S. Chern, *Prog. Polym. Sci*. **2006**, *31*, 443, https://doi.org/10.1016/j.progpolymsci.2006.02.001.
[20] P. A. Lovell, F. J. Schork, *Biomacromol*ecules **2020**, *21*, 4396, https://doi.org/10.1021/acs.biomac.0c00769.
[21] A. Böttcher, J. Petri, A. Langhoff, S. Scholl, W. Augustin, A. Hohlen, D. Johannsmann, *Macromol. React. Eng*. **2022**, *16*, 2100045, https://doi.org/10.1002/mren.202100045.
[22] J. Urrutia, J. M. Asua, *Ind. Eng. Chem. Res*. **2021**, *60*, 10502, https://doi.org/10.1021/acs.iecr.1c00097.
[23] J. M. Asua, *Macromol. React. Eng*. **2016**, *10*, 311, https://doi.org/10.1002/mren.201500032.
[24] J. M. Hoover, S. S. Stahl, *J. Am. Chem. Soc*. **2011**, *133*, 16901, https://doi.org/10.1021/ja206230h.
[25] J. M. Hoover, B. L. Ryland, S. S. Stahl, *J. Am. Chem. Soc*. **2013**, *135*, 2357, https://doi.org/10.1021/ja3117203.
[26] J. F. Greene, J. M. Hoover, D. S. Mannel, T. W. Root, S. S. Stahl, *Org. Process Res. Dev*. **2013**, *17*, 1247, https://doi.org/10.1021/op400207f.
[27] B. H. Lipshutz, M. Hageman, J. C. Fennewald, R. Linstadt, E. Slack, K. Voigtritter, *Chem. Commun*. **2014**, *50*, 11378, https://doi.org/10.1039/C4CC05163G.
[28] B. H. Lipshutz, S. Ghorai, A. R. Abela, R. Moser, T. Nishikata, C. Duplais, A. Krasovskiy, R. D. Gaston, R. C. Gadwood, *J. Org. Chem*. **2011**, *76*, 4379, https://doi.org/10.1021/jo101974u.
[29] V. Grignard, *Compt. Rend*. **1900**, *130*, 1322.
[30] M. Seeger, W. Otto, W. Flick, F. Bickelhaupt, O. S. Akkerman, in 'Ullmann's Encyclopedia of Industrial Chemistry', **2011**, https://doi.org/10.1002/14356007.a15_595.pub2.
[31] G. Menges-Flanagan, E. Deitmann, L. Gössl, C. Hofmann, P. Löb, *Org. Process Res. Dev*. **2020**, *24*, 315, https://doi.org/10.1021/acs.oprd.9b00493.
[32] M. Berton, K. Sheehan, A. Adamo, D. T. McQuade, *Beilstein J. Org. Chem*. **2020**, *16*, 1343, https://doi.org/10.3762/bjoc.16.115.
[33] L. Huck, A. de la Hoz, A. Díaz-Ortiz, J. Alcázar, *Org. Lett*. **2017**, *19*, 3747, https://doi.org/10.1021/acs.orglett.7b01590.
[34] E. Deitmann, K. Dahms, M. Maskos, D. Ziegenbalg, G. Menges-Flanagan, *Org. Process Res. Dev*. **2023**, 27, 2345, https://doi.org/10.1021/acs.oprd.3c00305.
[35] E. Deitmann, M. Maskos, G. Menges-Flanagan, D. Ziegenbalg, *React. Chem. Eng*. **2023**, *8*, 2717, https://doi.org/10.1039/D3RE00191A.
[36] M. E. Kopach, K. P. Cole, P. M. Pollock, M. D. Johnson, T. M. Braden, L. P. Webster, J. McClary Groh, A. D. McFarland, J. P. Schafer, J. J. Adler, M. Rosemeyer, *Org. Process Res. Dev*. **2016**, *20*, 1581, https://doi.org/10.1021/acs.oprd.6b00131.
[37] M. E. Kopach, D. J. Roberts, M. D. Johnson, J. M. Groh, J. J. Adler, J. P. Schafer, M. E. Kobierski, W. G. Trankle, *Green Chem.* **2012**, *14*, 1524, https://doi.org/10.1039/C2GC35050E.
[38] U. Tilstam, H. Weinmann, *Org. Process Res. Dev*. **2002**, *6*, 906, https://doi.org/10.1021/op025567+.
[39] H. Kryk, G. Hessel, W. Schmitt, N. Tefera, *Chem. Eng. Sci*. **2007**, *62*, 5198, https://doi.org/10.1016/j.ces.2007.01.013.
[40] D. J. am Ende, P. J. Clifford, D. M. DeAntonis, C. SantaMaria, S. J. Brenek, *Org. Process Res. Dev*. **1999**, *3*, 319, https://doi.org/10.1021/op9901801.

The definitive version of this article is the electronic one that can be found at https://doi.org/10.2533/chimia.2025.433